Transactions of the Korean Nuclear Society Autumn Meeting
Gyeongju, Korea, November 2-3, 2006

A Two-Step Diffusion Solution to the Doubly Heterogeneous PBMR-400 Problem

Hyun Chul Lee, Kang-Seog Kim, Jae Man Noh
Korea Atomic Energy Research Institute, 150 Deokjin-Dong, Yuseong-Gu, Daejeon, Korea, 305-353

1. Introduction

A strong spectral interaction between the core and the reflector has been one of the main concerns in the analysis of pebble bed reactor cores. To resolve this problem, we proposed a two-step procedure for the analysis of pebble bed reactor core and demonstrated the validity of the two-step procedure against a homogeneous PBMR-400 problem [1,2]. On the other hand, we also proposed Equivalent Cylinder Fuel Model (ECM) [3] to transform doubly heterogeneous spherical pebbles into singly heterogeneous cylindrical fuels by combining it with Reactivity-Equivalent Physical Transformation (RPT) [4].

In this study, we defined a doubly heterogeneous PBMR-400 benchmark problem and we presented a two-step diffusion solution to the problem as well as a Monte Carlo (MC) solution to the problem. In the first step of our two-step procedure, we used singly heterogeneous cylindrical fuel model for HELIOS[5] calculation, which was transformed from doubly heterogeneous spherical pebbles by combining ECM and RPT method. Results show an excellent agreement between the two-step diffusion solution and the MC solution.

2. Methods and Results

2.1 Benchmark Problem and the Reference Solution

A doubly heterogeneous benchmark problem derived from PBMR-400 reactor was introduced. Figure 1 shows the geometry and the dimensions of the problem. We assumed that the reflector region is homogeneous for simplicity while all the heterogeneities in the core region were considered. The temperature was assumed to be 300K everywhere. The packing fraction of pebbles in the core region was defined as 0.61. The number densities in each region of the problem are listed in Table 1. The reference solution to the doubly heterogeneous PBMR-400 benchmark problem was obtained from MC calculation by using the MC-CARD code. All the double heterogeneity including the coating layers were modeled explicitly in the MC model. Random packing was used for coated particle distribution in the fuel zone of pebbles while BCC packing was assumed for pebble distribution in the core region. No broken pebbles were allowed at the boundary of the core. A total of 451,352 pebbles were loaded in the core region and the resultant packing fraction in the core region was 0.60976. Figure 2 shows the radial packing fraction distribution. Sharp drops of radial packing fraction at the core boundaries are observed since no broken pebbles are allowed there.

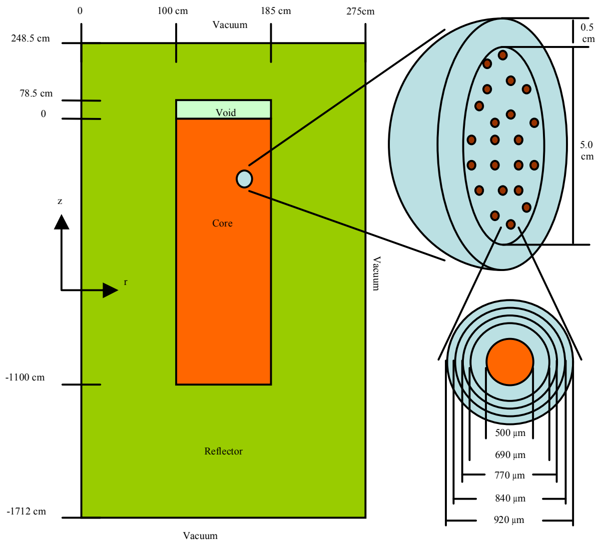

Figure 1. Geometry and dimensions of the problem

Table 1. Nuclide Number Densities in each region

Region	Nuclide	# Density (#/barn-cm)
UO_2 Kernel	U234 U235 U238 O16	1.18832E-05 1.35285E-03 2.18428E-02 4.64153E-02
Buffer Layer	C	5.26456E-02
Inner, Outer PyC Layer	C	9.52634E-02
SiC Layer	Si C	4.77600E-02 4.77600E-02
Reflector	C	9.02495E-02

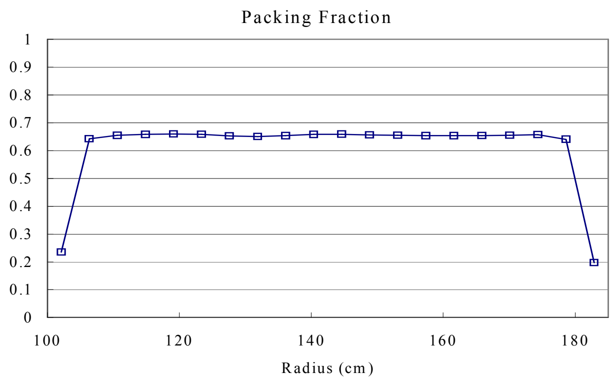

Figure 2. Radial Packing Fraction Distribution

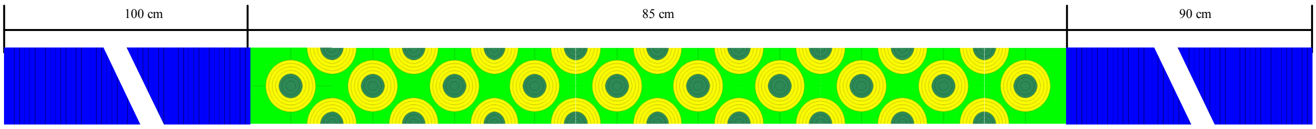

Figure 3. Infinite Slab Spectral Geometry Model for HELIOS

2.2 Spectral Geometry and Cross-section Generation

Figure 3 shows the infinite slab spectral geometry model for HELIOS calculation. The RPT radius of the pebble was determined so that the k_{eff} of HELIOS single cell calculation with ECM should be the same as that of doubly heterogeneous single cell MC calculation. The RPT radius determined in this way was 1.820cm and the corresponding radius of fuel region in ECM was 1.21333cm. We used the HELIOS code to generate 2-group cross sections for 11 spectral zones (9 spectral zones in the core). We obtained 2-group equivalent cross sections by applying the simplified equivalence theory [6].

2.3 Two-step Diffusion Solution to the Benchmark Problem

Table 2 compares the effective multiplication factor of MC calculation and that of two-step diffusion calculation. The difference is only 2 pcm. Figure 4 and 5 compare the radial and axial power distribution, respectively. We observe an excellent agreement between the two-step diffusion solutions and the MC solutions. We also observe sharp drops of radial power density at the core boundary which is not observed in a homogeneous core [1,2]. It is obvious that the drop in radial power density at the core boundary came from the radial packing fraction.

3. Conclusions

In this paper, we defined a doubly heterogeneous PBMR-400 benchmark problem and we presented a two-step diffusion solution to the problem. Results show an excellent agreement between the two-step diffusion solution and the Monte Carlo reference solution.

Acknowledgement

This study has been carried out under the Long-Term Nuclear R&D Program supported by the Ministry of Science and Technology (MOST) of Korea.

REFERENCES

1. Hyun Chul Lee et. al., "Two Step Procedure using a 1-D Slab Spectral Geometry in a Pebble Bed Reactor Core Analysis," Trans. Kor. Nucl. Soc. Autumn Mtg., Busan, Korea, Oct. 27-28, 2005.
2. Hyun Chul Lee, et. al., "Two Step Procedure by using a 1-D Slab Spectral Geometry for a Pebble Bed Reactor Core Analysis," PHYSOR 2006, Vancouver, BC, Canada, Sept. 10-14 2006.
3. Hyun Chul Lee et. al., "The Equivalent Cylinder Models for the Homogenization of Pebble Bed Reactor Cores," Trans. Am. Nucl. Soc. Vol. 93, Washington D.C., Nov. 13-17, 2005.
4. Y. Kim et. al., "Elimination of Double-Heterogeneity through a Reactivity-Equivalent Physical Transformation," GLOBAL 2005, Tsukba, Japan, Oct. 9-13, 2005.
5. J. F. Breismeister and et al., "MCNP–A General Monte Carlo N-Particle Transport Code, Version 4B," LA-12625-M (1997)
6. K. S. SMITH, "Spatial Homogenization Methods for Light Water Reactor Analysis," PhD Thesis, Massachusetts Institute of Technology (1980).

Table 2.Comparison of multiplication factors

MC-CARD		Two-step Diffusion	
k_{eff}	Std. dev.	k_{eff}	k_{eff} error
1.31486	17 pcm	1.31488	+2 pcm

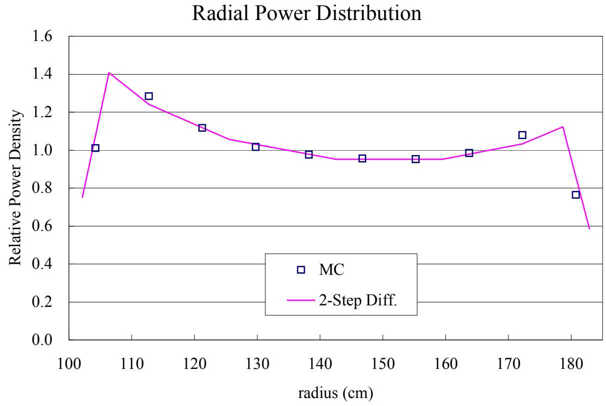

Figure 4. Comparison of Radial Power Density

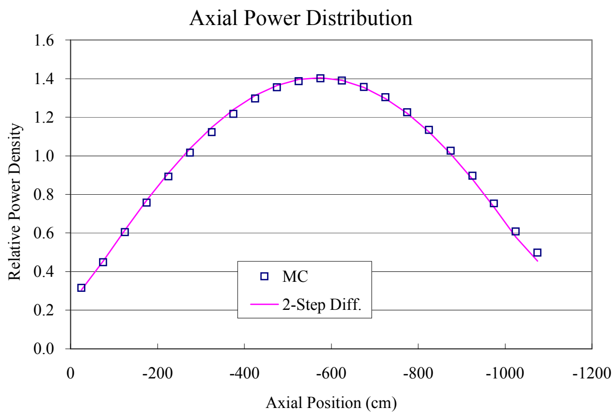

Figure 5. Comparison of Axial Power Density